Marmara Pharmaceutical Journal 21/2: XXX-XXX, 2017
DOI:

XX

Physicochemical, Thermal and Spectroscopic Characterization of Sodium Selenate Using XRD, PSD, DSC, TGA/DTG, UV-vis, and FT-IR

Mahendra Kumar Trivedi, Kalyan Kumar Sethi, Parthasarathi Panda, Snehasis Jana

ABSTRACT

Sodium selenate is an important inorganic compound, but lacks reliable and accurate physico-chemical and spectral characterization information. This article described the in-depth physicochemical, thermal, and spectroscopic characterization of sodium selenate using various analytical techniques. The powder X-ray diffractogram showed well-defined, narrow and sharp peaks revealed that sodium selenate is crystalline in nature. The crystallite size was found to be in the range of 28.75 to 49.97 nm. The average particle size was found to be of 3.93 (d_{10}), 14.44 (d_{50}), and 40.648 (d_{90}) µm with an average surface area of 0.676 m^2/g. The differential scanning calorimetry showed the endothermic inflation at 588.81 °C with the latent heat of fusion 103 J/g. The thermogravimetric analysis revealed two steps of the thermal degradation process. Similarly, the differential thermogravimetric analysis exhibited the major peaks in the thermogram and disclosed T_{max} at 852.65 °C. The UV-visible spectrum showed maximum absorbance at 205.1 nm (λ_{max}). This indicated sodium selenate thermally more stable in nature. The Fourier transform infrared spectrum showed a peak at 888 cm^{-1} due to the Se-O stretching. This information would be very much useful in the field of nutraceuticals/ pharmaceuticals and other industries using sodium selenate as an ingredient.

Key Words: Sodium selenate, Crystallite size, Particle size, Thermal analysis, Surface area

1. INTRODUCTION

Sodium selenate (Na_2SeO_4) is an important inorganic compound as a source of a trace essential nutritional element "selenium" and plays as an ingredient in multivitamins and livestock feeds (1-3). Selenium (Se) was investigated and observed to have the capability to delay the Alzheimer's symptoms as well as the initiation of skin aging (4, 5). It also protects various enzymes against the heavy metals toxicity such as Pb, Al, Cu, and Cd (6). Various other role of selenium on investigation found as an antioxidant (7), anti-cancer (8), and heart disease (4). Sodium selenate has the other applications in glass (8), pesticide, and some fungicides (9, 10) manufacturing industry. Chronic exposure or excessive dose of sodium selenate (1.6 mg/kg of body wt.) is toxic to human or animals and may cause severe lung, kidney, and liver damage (2, 3). Selenium (Se) bioavailability and toxicity depend on their chemical form or speciation. The toxicity of most forms of the selenium is low and sodium selenate exists in the highest +6 oxidation state, thus is stable under alkaline and other oxidizing conditions (11). Selenium is

Mahendra Kumar Trivedi
Trivedi Global, Inc., Henderson, Nevada-89052, USA

Kalyan Kumar Sethi, Parthasarathi Panda, Snehasis Jana
Trivedi Science Research Laboratory Pvt. Ltd., Bhopal-462026, Madhya Pradesh, India

Corresponding Author:
Snehasis Jana
e-mail: jana@trivedisrl.com

Submitted / Gönderilme: 00.00.0000 **Revised / Düzeltme:** 00.00.0000
Accepted / Kabul: 00.00.0000

more efficiently absorbed in the form of selenate than as selenite (94% versus 59%) (12).

Powder X-ray diffraction (PXRD), particle size distribution (PSD), differential scanning calorimetry (DSC), thermogravimetric/differential thermogravimetric analysis (TGA/DTG), ultraviolet-visible (UV-vis) spectroscopy, and Fourier transform infrared (FT-IR) spectrometry techniques can be used to solve the several problems experienced in the industries for pharmaceutical and/or nutraceutical formulation and development. To the best of our knowledge, a complete study on the physicochemical, thermal, and spectroscopic characterization of sodium selenate using these all techniques together is not yet reported, although sodium selenate has a wide range of applications in nutraceuticals, pharmaceuticals and other heavy industries (8-10, 12, 13). The physicochemical properties such as crystallite type and size, particle size, surface area, thermal properties, etc. that have the influence on its absorption, dissolution, and bioavailability have a lot of importance in formulation research and development (14). Therefore, the physico-chemical, thermal, and spectroscopic characterization of sodium selenate using PXRD, PSD, DSC, TGA/DTG, UV-Vis spectroscopy and FT-IR techniques were carried out and explored in-depth in this study.

2. MATERIALS AND METHODS

2.1 Chemicals

Sodium selenate was procured from Alfa Aesar, USA. All other chemicals used in the experiment were of analytical grade available in India.

2.2 Methods of analysis

The sodium selenate sample was evaluated using the various analytical techniques for its physicochemical and spectroscopic characterization.

2.2.1 Powder X-ray diffraction (PXRD) analysis

The XRD analysis was accomplished on PANalytical X'pert Pro powder X-ray diffractometer system. The X-ray of wavelength (λ) 1.54056 Å was used. The data were collected in the form of a chart of the Bragg angle (2θ) *vs.* intensity (counts/second), and a detailed table containing information on peak intensity counts, d-value (Å), relative intensity (%), full-width half maximum (FWHM) (θ°) (Table 1). From the XRD results, the crystallite size (G) was calculated using X'pert data collector and X'pert high score plus processing software. The method was based on the width of the diffraction patterns obtained in the X-ray reflected the crystalline region. The crystallite size (G) was calculated by using the following Scherrer formula (15, 16):

$$G = k\lambda/(b\text{Cos}\theta)$$

Where, k is the equipment constant (0.5), λ is the X-ray wavelength (0.154 nm); b in radians is the FWHM of the peak and θ the corresponding Bragg angle.

The sample was prepared using 500 mg of sodium selenate. The sample holder ring was fixed to the sample preparation table, and the sample was prepared by back loading technique using sample preparation kit. Then it was spread with sufficient quantity in the holder ring to fill the ring cavity. The sample was pressed down using powder press block, and the surplus powder was scraped using a glass slide to get a densely packed specimen. The bottom plate was positioned onto the holder ring and clamp in position. The sample holder was removed from the sample preparation table by turning it upside down. A smooth surface of the sample was obtained to ensure the optimum results (16).

Table 1: Powder X-ray diffraction data with Bragg angle, d-spacing, relative intensities, areas, and crystallite size analysis of sodium selenate.

Bragg angle (°2θ)	d-spacing (Å)	Rel. Int. (%)	FWHM (°2θ)	Area (cts*°2θ)	Crystallite size (G, nm)
18.43	4.81	100.00	0.1004	1614.89	44.42
22.55	3.94	17.14	0.1004	276.84	44.71
27.3	3.27	40.91	0.1004	661.16	45.12
28.43	3.14	29.29	0.1338	630.58	33.94
31.05	2.88	55.29	0.1004	892.81	45.51
32.68	2.74	75.34	0.1338	1622.17	34.29
37.26	2.45	21.45	0.1171	404.18	39.68
47.4	1.92	20.15	0.1673	542.45	28.75
48.84	1.86	11.40	0.1338	245.51	36.15
52.99	1.73	31.83	0.1004	514.04	49.02
57.2	1.61	14.37	0.1004	232.06	49.97
68.31	1.37	9.84	0.1224	261.91	43.50
Average				658.23	41.25

Rel. Int.: Relative intensity; FMHM: Full width at half maximum.

2.2.2 Particle size distribution (PSD) analysis

The average particle size and particle size distribution were analyzed using Malvern Mastersizer 2000, UK with a detection range between 0.01 µm to 3000 µm. The sample was prepared with 0.15 g of sodium selenate added with 2 drops of span 85 and 10 mL of sunflower oil. The suspension was mixed with the mixer for 2 minutes. The sample unit was filled with the dispersant medium (sunflower oil) and operated the stirrer at 2500 rpm. Alignment of the optics was done and taken the background measurement. After the background measurement, the sample was added to the sample unit with constant monitoring the obscuration and stopped the addition of sample when the obscuration reached in between 10 and 20%. When the obscuration was stable, the measurement was taken six times. The histograms of the measurement were recorded. The particle size (µm) for at below 10% level (d_{10}), 50% level (d_{50}), and 90% level (d_{90}) were calculated from the histogram (17) and presented in Table 2. The calculations were done by using software Mastersizer 2000.

One common measure of the cumulative distribution is the span (d_{90} - d_{10}), and the relative span is a common calculation to quantify distribution width: (18, 19)

$$\text{Relative span} = (d_{90} - d_{10})/d_{50}$$

Table 2: Particle-size distribution (d_{10}, d_{50} and d_{90}) and surface area analysis of sodium selenate.

Measurement	d_{10} (µm)	d_{50} (µm)	d_{90} (µm)	Surface area (m^2/g)
1	4.01	15.06	46.81	0.65
2	3.95	14.58	41.47	0.67
3	3.91	14.26	38.85	0.68
4	3.91	14.22	38.65	0.68
5	3.89	14.09	37.76	0.69
6	3.93	14.43	40.35	0.68
Average	3.93	14.44	40.65	0.68

2.2.3 Differential scanning calorimetry (DSC)

The thermal properties of sodium selenate were analyzed using the DSC Q20 (TA instruments, USA) differential scanning calorimeter. 2.70 mg of sample was weighed and sealed in aluminium pans and equilibrated at 25 °C. Then the sample was heated up to 600 °C at the heating rate of 10 °C/min under nitrogen gas as purge atmosphere with a flow rate of 50 mL/min. The values of onset, endset, peak temperature, peak height (mJ or mW), peak area, and change in heat (J/g) for each peak were recorded.

2.2.4 Thermogravimetric /Derivative thermogravimetric analysis (TGA/DTG)

The TG analysis was performed using instruments TGA Q50 (TA instruments, USA) at a heating rate of 10 °C/min from room temperature, *i.e.* 25 °C to 900 °C under a nitrogen atmosphere (sample mass 11.86 mg on a platinum pan). In TGA, the weight loss for each step was recorded in grams as well as the percent loss with respect to the initial weight along with, the onset, endset, and peak temperature for each step were recorded. Similarly, in DTG, the onset, endset, peak temperature, and change in heat (J/g) of each peak were recorded.

2.2.5 Ultra violet-visible spectroscopy (UV-Vis) analysis

The UV-vis spectroscopic analysis of sodium selenate was carried out using Shimadzu UV-2450 (Shimadzu, Japan) with UV probe. The spectrum was recorded using 1 cm quartz cell that has a slit width of 1.0 nm. The wavelength ranges chosen for recording the spectrum were 190-800 nm. The absorbance spectrum (in the range of 0.2 to 0.9) and absorbance maximum (λ_{max}) were recorded.

2.2.6 Fourier transform infrared (FT-IR) spectroscopy

FT-IR spectroscopy of sodium selenate was performed on Spectrum two (Perkin Elmer, USA) Fourier transform infrared spectrometer with the frequency array of 400-4000 cm^{-1} by using pressed KBr disk technique. The compound was run as pressed disks using 300 mg of KBr as the diluents and 2.06 mg of sodium selenate sample.

3. RESULTS AND DISCUSSION

3.1 Powder X-ray diffraction (PXRD) analysis

Powder X-ray diffraction provides the characteristic diffraction pattern from the powder material which is often easier and more convenient method than individual crystal diffraction (20). The diffractogram of sodium selenate showed the XRD patterns (Figure 1). The intensity data were in Bragg's angle (2θ) range of 10-100° (Figure 1). The PXRD

patterns showed well-defined, narrow, sharp, significant peak at 2θ position equal to 18.43, 22.55, 27.30, 28.43, 31.05, 32.68, 37.26, 47.40, 48.84, 52.99, 57.2, and 68.31°. This observation represented the crystalline nature sodium selenate. The d-spacing obtained are 4.81, 3.94, 3.27, 3.14, 2.88, 2.74, 2.45, 1.92, 1.86, 1.73, 1.61, and 1.37 Å (Table 1), which help in identification of sodium selenate, because each compound has a set of unique d-spacing (21, 22). The d-spacing are in the range of 4.81 to 1.37 Å and decreased with increased 2θ values. Typically, this could be a set of standard d-spacing information in order to achieve the identification of the unknown samples.

The peak intensity (I) was reported as peak height intensity (Table 1) and the relative intensity was recorded as the ratio of the peak intensity to that of the strongest peak (I_1) (relative intensity = I/I_1 x 100). The integrated peak intensities also calculated and the average peak area calculated for the sodium selenate was 61.846 (Table 1). The relative peaks intensities could be altered due to the texture (*i.e.* preferred crystallographic orientation) in the sample (23).

The full-width half maximum (FWHM) is a very important factor for the calculation of crystallite size using the Scherrer equation ($G = k\lambda/bCos\theta$) (15). The crystallite size was found to be in the range of 28.75 to 49.97 nm (Table 1). The average crystallite size of sodium selenate was calculated to be 41.25 nm (Table 1). Crystal lattice strain has the impact on the crystallite size (20). However, the PXRD analysis of sodium selenate is a rapid, non-destructive important technique and these data would be much useful in all stages of nutraceuticals, and pharmaceuticals research and development.

3.2 Particle size distribution (PSD) analysis

The particle size of sodium selenate was investigated, and the results are presented in Table 2. The distribution width cited three values on the X-axis, the d_{10}, d_{50}, and d_{90} diameter as shown in Figure 2. The experiment was repeated for six-time, and the average of particle size and surface area were calculated from the data (Table 2). The average particle size of the sodium selenate powder sample was 3.93 (d_{10}), 14.44 (d_{50}), and 40.65 μm (d_{90}) (Table 2). The PSD analysis indicated the average surface area of sodium selenate of 0.676 m^2/g (Table 2). Surface area and energy of a particle play an important role in the dissolution of a formulation in a medium/solvent. The calculated span value was to be 36.71 μm, and relative span value was 2.54 particularly for this sodium selenate powder. The significance of the span value describes relative dispersion and could be applied to all particle distributions, and deviations often under d_{10} and over d_{90} (19, 20). The particle size distribution and its area play a significant role in nutraceuticals/pharmaceutical formulation development and research (24).

3.3 Differential scanning calorimetry (DSC) analysis

The thermal analysis of sodium selenate provided the decomposition temperature and latent heat of fusion and the

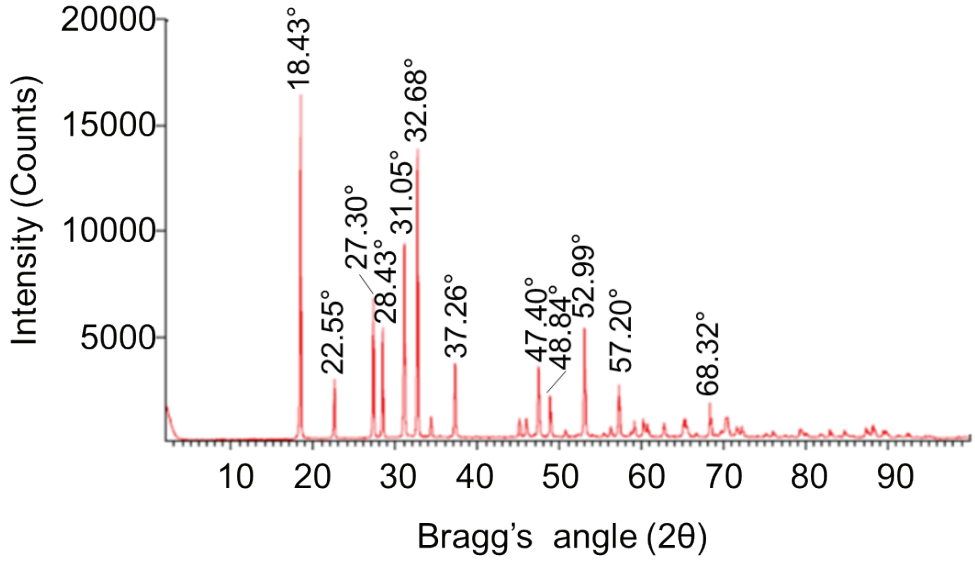

Figure 1: Powder X-ray diffraction patterns of sodium selenate.

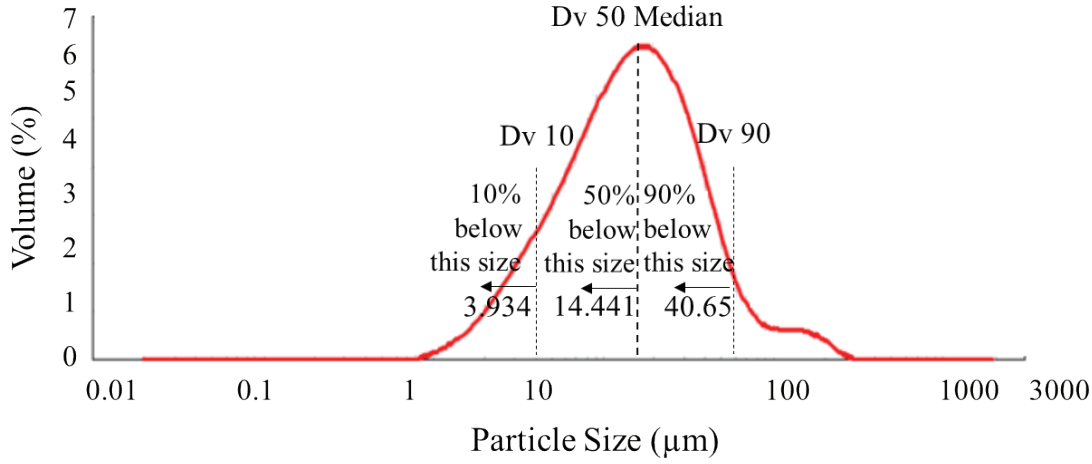

Figure 2: Particle size distribution (d_{10}, d_{50}, and d_{90}) histogram of sodium selenate.

results are presented in Figure 3. The DSC thermogram of sodium selenate represented a very sharp endothermic peak at 588.81 ºC and the ΔH fusion was about 103 J/g. The onset, peak, and endset temperature to the latent heat of fusion was 584.41, 588.81, and 596.19 ºC, respectively. The enthalpy of melting/fusion is the heat energy required for melting, *i.e.* for breaking down the sodium selenate crystalline lattice. The absence of glass transition temperature in the DSC thermogram proved the crystal nature of sodium selenate (25).

3.4 Thermogravimetric /Derivative thermogravimetric analysis (TGA/DTG)

The TGA and DTG thermograms of sodium selenate are shown in Figures 4a and 4b, respectively. The TGA analysis revealed the changes in physical and chemical properties of sodium selenate as a function of increasing temperature. The TGA thermogram showed two steps of thermal degradation process (Figures 4a). The sodium selenate sample had lost 0.14% (0.013 mg) and 6.73% (0.657 mg) in the first and second step of degradation respectively, of their total original weight (Figure 4a). The major weight loss was in the second step of degradation in the temperature range of 101.01 to 896.18 °C. The result indicated sodium selenate was highly thermally stable compound due to inorganic in nature.

The DTG analysis exhibited one small and one major peak in the thermogram (Figure 4b) of sodium selenate. The peak at 97.48 °C might be due to the trapped water during the experimentation, which was supported by the DSC and TGA data. The maximum temperature (T_{max}) was at 852.65 °C. The onset, peak, and endset temperature were 757.89, 852.65, and 896.18 °C, respectively. These results indicated that sodium selenate is thermally stable compound for higher temperature (i.e. 852.65 °C). These data would be helpful for pharmaceuticals/nutraceuticals and other industries dealings with sodium selenate (26-27).

3.5 Ultra violet-visible spectroscopy (UV-Vis) analysis

The UV-visible spectrum of sodium selenate is shown in Figure 5. It has been reported that the UV absorbance occurred due to the excitation of electrons from highest energy occupied molecular orbital (HOMO) to lowest energy unoccupied molecular orbital (LUMO) (28). The UV spectrum of the sodium selenate sample exhibited the maximum absorbance at 205.1 nm (λ_{max}). The λ_{max} at 205.1 nm was indicated the absorbance maxima of 2.5628. The information of UV-visible characterization data would be helpful in analytical chemistry for the qualitative and quantitative analysis of the analyte in samples containing sodium selenate.

3.6 Fourier transform infrared (FT-IR) spectroscopy

The FT-IR spectrum of sodium selenate is presented in Figure 6. The spectrum showed a broad peak at 3541 cm^{-1} and 1723 cm^{-1} might be due to the O-H stretching and bending vibration respectively, due to the trapped water molecule, which is incorporated into the lattice structure

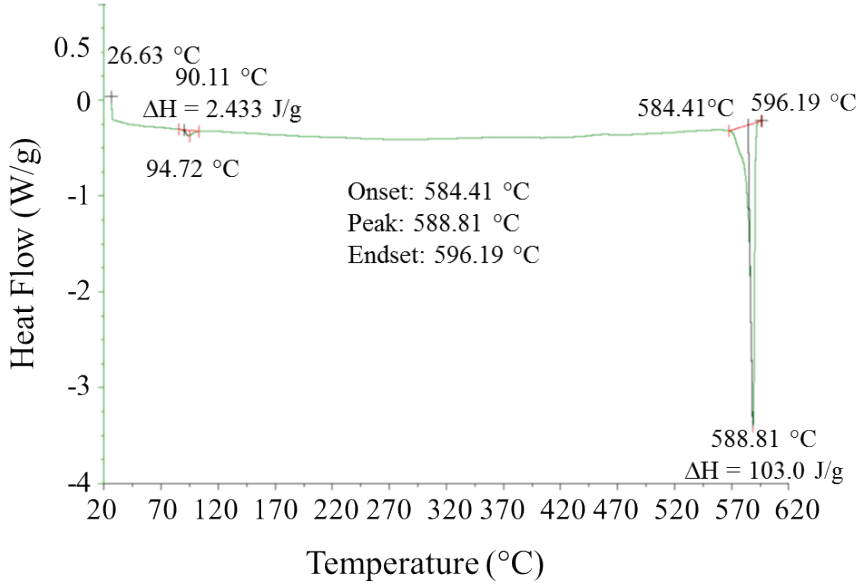

Figure 3: DSC thermogram is representing the decomposition temperature (°C) and latent heat of fusion (ΔH in J/g) of sodium selenate.

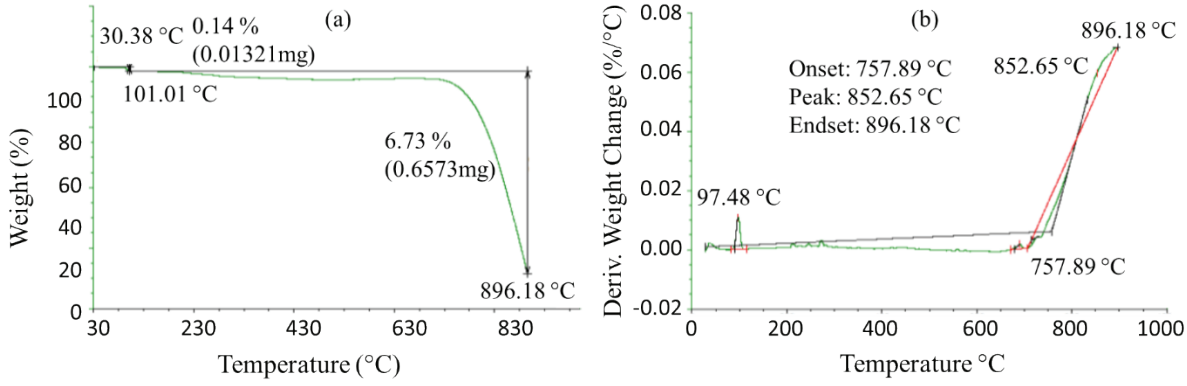

Figure 4: TGA (a) and DTG (b) thermograms of sodium selenate showing the degradation steps and temperature.

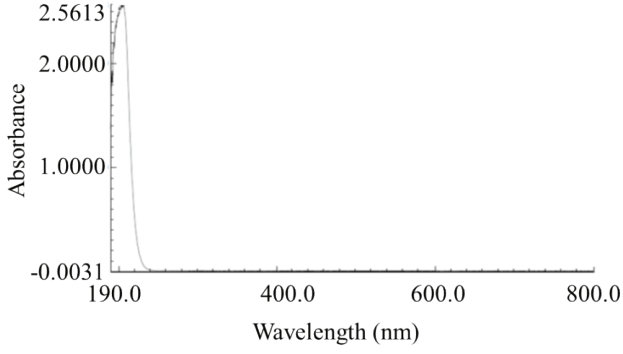

Figure 5: UV-vis spectrum of sodium selenate.

of the crystalline inorganic compounds and produced the characteristic absorption bands. The information was supported by the DSC, TGA, and DTG analysis report. The spectrum showed the strong and sharp peak at 888 cm^{-1} (Figure 6) due to the Se-O stretching in the fingerprint region of sodium selenate. The pattern of the spectrum was closely matched with the reported literature (29). The characteristic FT-IR spectroscopic information would be helpful in order to quick, qualitative establishment of sodium selenate in various samples.

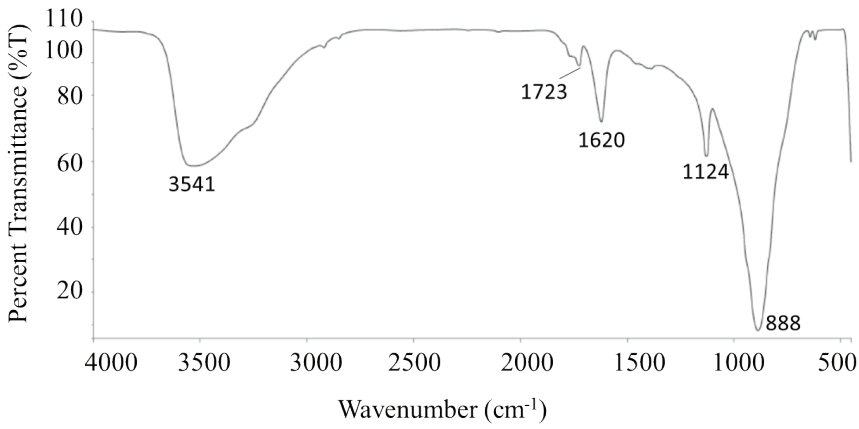

Figure 6: Fourier transform infrared (FT-IR) spectrum of sodium selenate.

4. CONCLUSIONS

The current study effectively investigated in-depth physicochemical, and spectroscopic characterization of sodium selenate using XRD, PSD, DSC, TG/DTG, UV-vis, and FT-IR analytical technique. The sodium selenate PXRD patterns showed significant narrow, and sharp; peak at Bragg's angle (2θ) position, indicated the crystalline nature of sodium selenate. The crystallite size was found to be in the range of 28.75 to 49.97 nm. The average particle size of sodium selenate was 3.93 (d_{10}), 14.44 (d_{50}), and 40.65 µm (d_{90}) and average surface area of 0.676 m^2/g. The calculated span and relative span value were 36.71 µm and 2.54, respectively. The DSC thermogram of sodium selenate showed endothermic inflation at 588.81 **°C.** The overall thermal characterization indicated sodium selenate has the long range melting/degradation temperature implies very high thermal stability. The UV-visible spectrum showed the highest absorbance maxima (λ_{max}) at of 205.1 nm. The FT-IR spectrum showed the strong and sharp peak at 888 cm^{-1} due to the Se-O stretching. These in-depth, comprehensive, physico-chemical and thermal solid state characterization information of sodium selenate would be a useful asset. This can set a standard for scientific qualitative and quantitative analysis of nutraceuticals, pharmaceuticals and other industries utilizing sodium selenate as an ingredients.

5. ACKNOWLEDGEMENT

The authors gratefully acknowledged to GVK Biosciences Pvt. Ltd., Hyderabad, India for their support.

6. CONFLICT OF INTEREST

Authors confirm that this article content has no conflict of interest.

Sodyum selenat'ın XRD, PSD, DSC, TGA/DTG, UV-VIS ve FT-IR yöntemleri ile fizikokimyasal, termal ve spektroskopik karakterizasyonu

ÖZ

Önemli bir inorganik bileşik olan sodium selanat'ın fizikokimyasal ve spektral yöntemlerle karakterizasyonuna dair kesin ve güvenilir veri bulunmamaktadır. Bu makale, sodium selenat'ın çeşitli analitik yöntemler kullanılarak yapılan fizikokimyasal, termal ve spektroskopik karakterizasyonu ile ilgili geniş kapsamlı veri içermektedir. Toz X-ışını difraksiyonu verileri incelendiğinde görülen dar ve keskin pikler sodium selenat'ın doğal billurî yapısına işaret etmektedir. Kristalit boyutu 28.75 - 49.97 nm aralığında bulunmuştur. Ortalama partikül boyutu 3.93 (d_{10}), 14.44 (d_{50}), ve 40.648 (d_{90}) µm, ortalama yüzey alanı 0.676 m^2/g'dır. Diferansiyel taramalı kalorimetre kullanılarak yapılan çalışmalarda 588.81 °C'de endotermik şişkinlik gösteren sodium selenat'ın gizil füzyon ısısı 103 J/g olarak tespit edilmiştir. Termogravimetrik çalışmalar, sodium selenat'ın termal bozunma sürecinin iki basamaklı olduğunu göstermiştir. Benzer şekilde, diferansiyel termogravimetrik analizlerde de termogramda iki ana pik ve 852.65 °C'de T_{max} tespit edilmiştir. Bileşiğe ait UV-VIS spektrumunda maksimum absorbans 205.1 nm (λ_{max})'de tespit edilmiştir. Bu veriler, sodium selenat'ın doğada termal olarak kararlı olduğunu göstermektedir. FT-IR spektrumunda, 888 cm^{-1}'de Se-O gerilme titreşimlerine atfedilen bir band görülmüştür. Elde edilen bu bilgilerin, nutrasötik / farmasötik ve sodium selenat'ın bir bileşen olarak kullanıldığı diğer endüstri dalları için de faydalı olduğu düşünülmektedir.

Anahtar Kelimeler: Sodyum selenat, Kristalit boyutu, Parçacık boyutu, Termal analiz, Yüzey alanı

REFERENCES

1. Martens DA. Selenium. In: Encyclopedia of Water Science. United States Department of Agriculture (USDA), Tucson, Arizona, USA. 2003.
2. Stadlober M, Sager M, Irgolic K. Identification and quantification of selenium compounds in sodium selenite supplemented feeds by HPLC-ICP-MS. Die Bodenkultur 2001; 52: 233-41.
3. Ganther HE, Baumann CA. Selenium metabolism. II. Modifying effects of sulfate. J Nutr 1962; 77: 408-14.
4. Cardoso BR, Ong TP, Jacob-Filho W, Jaluul O, Freitas MI, Cozzolino SM. Nutritional status of selenium in Alzheimer's disease patients. Br J Nutr 2010;103: 803-6.
5. Chen J, Berry MJ. Selenium and selenoproteins in the brain and brain diseases. J Neurochem 2003; 86: 1-12.
6. Ani M, Moshtaghie AA, Aghadavod M. Protective effects of selenium and zinc on the brain acetylcholinesterase activity in lead intoxified rat. Res Pharm Sci 2007; 2: 80-4.
7. Abubakar MG, Taylor A, Ferns GA. The effects of aluminium and selenium supplementation on brain and liver antioxidant status in the rat. Afr J Biotechnol 2004; 3: 88-93.
8. Fleet JC. Dietary selenium repletion may reduce cancer incidence in people at high risk who live in areas with low soil selenium. Nutr Rev 1997; 55: 277-9.
9. Krieger RI. Handbook of pesticide toxicology, 2nd edition, volume 1. Academic Press. San Diego. 2001, pp. 1908.
10. Hanson B, Lindblom SD, Loeffler ML, Pilon-Smits EAH. Selenium protects plants from phloem-feeding aphids due to both deterrence and toxicity. New Phytol 2004; 162: 655-62.
11. Barceloux DG, Barceloux D. Selenium. J Toxicol Clin Toxicol 1999; 37: 145-72.
12. Thomson CD, Robinson MF. Urinary and fecal excretions and absorption of a large supplement of selenium: Superiority of selenate over selenite. Am J Clin Nutr 1986; 44: 659-63.
13. Salama RM, Schaalan MF, Elkoussi AA, Khalifa AE. Potential utility of sodium selenate as an adjunct to metformin in treating type II diabetes mellitus in rats: A perspective on protein tyrosine phosphatase. Biomed Res Int 2013; 231378.
14. Chereson R. Bioavailability, bioequivalence, and drug selection. In: Basic pharmacokinetics, 1st edition. Editors: Makoid CM, Vuchetich PJ, Banakar UV Pharmaceutical Press. London. 2009.
15. Langford JI, Wilson AJC. Scherrer after sixty years: A survey and some new results in the determination of crystallite size. J ApplCryst 1978; 11: 102-13.
16. Buhrke VE, Jenkins R, Smith DK. Preparation of specimens for X-ray fluorescence and X-ray diffraction analysis. John Wiley & Sons Inc. New York. 1998, pp. 148.
17. Burgess DJ, Duffy E, Etzler F, Hickey AJ. Particle size analysis: AAPS workshop report, cosponsored by the Food and Drug Administration and the United States Pharmacopeia. AAPS J 2004; 6: 23-34.
18. Weiner BB. What is a continuous particle size distribution? Brookhaven Instruments, NY, USA. 2011.
19. Wolfrom RL The language of particle size. J GXP Compliance 2011; 15: 10-20.
20. Balzar D, Audebrand, Daymond MR, Fitch A, Hewat A, Langford JI, Le Bail A, Louër D, Masson O, McCowan CN, Popa NC, Stephens PW, Toby HB. Size-strain line-broadening analysis of the ceria round-robin sample. J Appl Crystallogr 2004; 37: 911-24.
21. Swanson HE, McMurdie HF, Evans MCME, Paretzkin B, DeGroot JH, Carmel SJ.Standard X-Ray Diffraction Powder Patterns. National Bureau of Standards Monograph-25, Section 9, Nat Bur Stand 1971. pp. 55.
22. Moore DM, Reynolds Jr RC. X-Ray diffraction and the identification and analysis of clay mineral, 2nd edition. Oxford University Press. New York. 1997.
23. Sardela M. X-ray Analysis Methods. Advanced Materials Characterization Workshop, The Frederick Seitz Materials Research Laboratory-University of Illinois at Urbana-Champaign. 2008.
24. Martin AN, Patrick JS. Martin's physical pharmacy and pharmaceutical sciences: Physical chemical and biopharmaceutical principles in the pharmaceutical sciences. Phila: Lippincott Williams and Wilkins. 2006.
25. Jones AT. Development of the γ-crystal form in random copolymers of propylene and their analysis by DSC and X-ray methods. Polymer 1971; 12: 487-508.
26. Martin FJ, Albers H, Lambeck PV, Van de Velde GMH, Popma ThJA. Luminescent thin films by the chemical aerosol deposition technology (CADT). J Aerosol Sci 1991; 22: 435-8.
27. Bajaj S, Singla D, Sakhuja N. Stability testing of pharmaceutical products. J Appl Pharm Sci 2012; 2: 129-38.
28. Bansal KR. Synthetic Approaches in Organic Chemistry. Jones & Bartlett Publishers International. 1998, pp. 236.
29. Miller FA, Wilkins CH. Infrared spectra and characteristic frequencies of inorganic ions their use in qualitative analysis. Anal Chem 1952; 24: 1281.